Synthesis of poly-2-hydroxyethyl methacrylate–montmorillonite nanocomposite via in situ atom transfer radical polymerization

Ayhan Oral[a)]
Department of Chemistry, Faculty of Arts and Science, Çanakkale Onsekiz Mart University, Çanakkale-17100, Turkey; and Department of Chemistry, Faculty of Science, Ege University, İzmir-Turkey

Talal Shahwan
Department of Chemistry, İzmir Institute of Technology, 35430 Urla, İzmir-Turkey

Çetin Güler
Department of Chemistry, Faculty of Science, Ege University, İzmir-Turkey

(Received 17 April 2008; accepted 13 August 2008)

The poly-2-hyroxyethyl methacrylate (PHEMA)/clay nanocomposite was synthesized by in situ atom transfer radical polymerization (ATRP) from initiator moieties immobilized within the silicate galleries of the clay particles. To produce organically modified montmorillonite (MMT) that has ATRP initiator moiety, a new catalyst that consists of quaternary ammonium salt moiety and an initiator moiety was synthesized. This initiator was intercalated into the interlayer spacing of the MMT. The polymerization reaction was carried out in a mixed solvent system consisting of methyl ethyl ketone and 1-propanol at 50 °C, using the initiator that has been already synthesized with a copper bromide catalyst. The 2, 2′-bipyridyl (bpy) complex was used as ligand. The products were characterized via Fourier transform infrared, nuclear magnetic resonance (^{1}H NMR, ^{12}C NMR), transmission electron microscopy, x-ray diffraction, thermogravimetric analysis, and differential scanning calorimetry.

I. INTRODUCTION

During the last decade, intensive research has been carried out in the field of polymer nanocomposites. Within this context, various filling materials are introduced into polymer matrices to improve the physical, thermal, and chemical properties of these polymers and reduce their cost.

The field of polymer/layered silicate (PLS) nanocomposites has gained momentum recently as small amounts of layered silicate loadings resulted in pronounced improvements in the performance of the modified polymers, in comparison to virgin polymers or conventional micro- and macrocomposites.[1–12]

In polymer-clay nanocomposites, the distribution and ordering of the clay particles or layers in the polymer matrix determines the characteristics of the nanocomposite. In general, two idealized structures of the polymer-clay composites can be achieved: intercalated and exfoliated structures. An exfoliated structure consists of individual nanometer-thick silicate layers dispersed in a polymer matrix resulting from extensive polymer penetration and delaminating of the silicate layers. Limited polymer penetration results in finite expansion of the silicate layers in the intercalated structure. This leads to increasing the *d*-spacing by a few nanometers and thereby produces intercalated hybrids that consist of well-ordered multilayers with alternating polymer/silicate layers. In practice, many systems fall short of the idealized exfoliated morphology. More commonly, partially exfoliated nanocomposites contain small stacks of 2 to 4 layers uniformly dispersed in the polymer matrix.[13]

Nanocomposites can be prepared by various methods, such as in situ polymerization, polymer melt intercalation/exfoliation, solution intercalation/exfoliation, and sol-gel synthesis.[14–26] In situ intercalative polymerization methods have some advantages that include producing a nanocomposite with predictable molecular weights and low polydispersities. Among the studies available in literature in this field is the work of Weimer et al.,[21] who used nitroxide-mediated polymerization to produce a polystyrene (PS)-montmorillonite (MMT) nanocomposite. Alternatively, Böttcher et al.,[22] used atom transfer radical polymerization (ATRP) to synthesize poly(methyl methacrylate) (PMMA)–MMT nanocomposites, and Zhou et al.,[26] studied surface-initiated anionic polymerization of styrene on MMT.

[a)]Address all correspondence to this author.
e-mail: ayhan1oral@yahoo.com
DOI: 10.1557/JMR.2008.0396

The main aim of this work is to synthesis the polymer-MMT nanocomposite via in situ intercalative polymerization method. This work is divided into two parts, the first part deals with the synthesis and characterization of difunctional initiator that consists of quaternary ammonium salt moiety and an initiator moiety. The second part includes the synthesis and characterization of nanocomposite. After the initiator was synthesized and then penetrated into galleries of the MMT, the polymerization process was carried out by in situ ATRP according to the procedure reported by Beers et al.[27]

II. EXPERIMENTAL

A. Materials

MMT K-10 (Sigma-Aldrich, Steinheim, Germany), 6-amino haxanol (Fluka, Steinheim, Germany), triethylamine (Sigma-Aldrich), dibenzoyl peroxide, acetone, dichloromethane (DCM), dibenzoyl peroxide $(BzO_2)_2$, and 2-bromoisobutyryl bromide (Sigma-Aldrich) was vacuum distilled. Methyl ethyl ketone (MEK) and 1-propanol were purified by distillations. The 2, 2′-bipyridine (bpy) from Aldrich was recrystallized from *n*-hexane to remove impurities. CuBr was washed with acetic acid followed by methanol to remove impurities.

The monomer was purified by washing an aqueous solution (25 vol% HEMA) of the monomer with hexanes (4 × 200 mL), salting the monomer out of the aqueous phase by addition of NaCl, drying over $MgSO_4$, and distilling under reduced pressure.

B. Initiator synthesis

The initiator synthesis was carried out in two steps. In the first step, the quaternization of amine group was realized (Fig. 1). For this purpose, 1.5 g 6-aminohexanol (14.6 mmol) was dissolved in 20 mL DCM in a Schlenk tube and kept in Ar atmosphere. Saturated ether-HCl solution was added dropwise to the solution. This mixture was stirred for 3 h. The formed HCl salt was filtered out and washed three times with a total of 50 mL of cold diethylether. The residual solvent was removed in vacuum, and the yellowish product was separated.

In the second step, the esterification of 6-hydroxyhexan-1-aminium chloride with 2-bromo-isobutyryl bromide was realized (Fig. 2). For this purpose, 1.4 g of product 1 (13.7 mmol) was dissolved in 10 mL anhydrous acetone. The resulting solution was cooled in an ice bath and stirred for 2 h. Meanwhile, 2-bromoisobutyryl bromide (1.7 mL, 13.7 mmol) was dissolved in 5 mL anhydrous acetone. This solution was then transferred to a dropping funnel and was dropwise added over a 3 h period. After stirring the mixture for 20 h, the solvent was evaporated. The final product was dissolved again in acetone and precipitated in diethylether. The product was isolated with 71% yield.

The data relevant to the synthesized initiator are represented as below; ^{1}H NMR ($CDCl_3$, 300 MHz) 7.95 (s, 3H, NH_3), d 4.17 (t, 2H, CH_2O), 3.07 (m, 2H, CH_2N), 1.79 [s, 6H, $(CH_3)_2$], 1.74 (m, 2H, CH_2), 1.73 (m, 2H, CH_2), 1.68 [m, 4H, $(CH_2)_2$] ^{13}C NMR (300 MHz) d 171.6 (RCOOR), 65.0 (CH_2O), 52.0 [$(CH_3)_2CBr$], 40.5 (N–CH_2), 30.5 [$(CH_3)_2$], 28.3, 26.7, 25.2, 19.7, (CH_2); Fourier transform infrared (FTIR) 2852 (N^+), 1736 (C = O).

C. Modification of clay

The initiator was ion-exchanged onto MMT (Fig. 3). For this purpose, 1.0 g of MMT was dispersed into

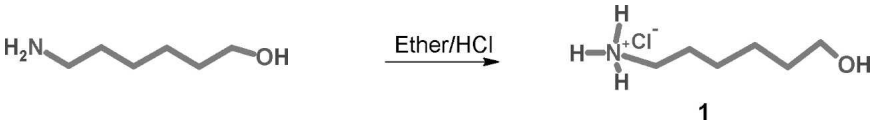

FIG. 1. Step 1 of initiator synthesis.

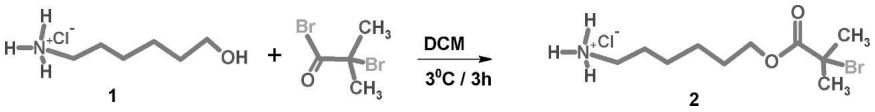

FIG. 2. Step 2 of initiator synthesis.

FIG. 3. The cation-exchange process (curves represent the backbones of the initiator 2, spheres represent quaternary ammonium moiety of the initiator 2, capsules represent initiating group, and stars represent exchangeable cations).

50 mL acetone at room temperature and the suspension was stirred for 30 min. A 0.3 g sample of the 6-[(2-bromo-2-methylpropanoyl) oxy] hexan-1-aminium chloride was added into the MMT-acetone dispersion under vigorous stirring. Stirring was continued for 4 h, and the mixture was then left without stirring for an additional 12 h. The exchanged clay was filtered and washed twice with acetone to remove adsorbed molecules. It was then dried in vacuum at room temperature.[23] The amount of immobilized initiator was determined by thermogravimetric analysis (TGA) to be 0.63 mequiv immobilized initiator/g MMT.

D. Polymerization of HEMA

Two types of the polymerization methods were used to synthesize the poly-2-hyroxyethyl methacrylate (PHEMA); the first is radical polymerization with dibenzoylperoxide, and the second is polymerization via ATRP.

(i) Free radical polymerization of HEMA: After 3.0 mL of HEMA was dissolved in 15 mL of the solvent (70/30 v/v MEK/1-propanol), 0.024 g of dibenzoylperoxide was added to this solution. This solution was stirred at room temperature for 0.5 h. The temperature was increased from room temperature to 80 °C and the solution was stirred for 2 h. The resulting product was finally precipitated in diethylether two times.

(ii) ATRP of HEMA without MMT: The polymerization process was carried out according to the procedure reported by Beers et al.,[27] but instead of modified MMT only the initiator was used.

(iii) Effect of MMT (K10) for polymerization of HEMA: Another polymerization attempt was tried to reveal the effect of MMT (K10) on the polymerization at the same condition of the previous ATRP process. This step did not include the initiator, ligand, and CuBr. It included only the monomer, the solvent, and MMT (K10). According to the results, the clay did not affect the polymerization of HEMA under the given conditions.

E. Nanocomposite synthesis

As noted earlier, the polymerization process was carried out according to the procedure reported in the literature.[27] In a typical polymerization process, all reactions were carried out in Schlenk flasks magnetic stirring. First, a 10 mL Schlenk flask was charged with 0.19 g MMT modified with catalyst (0.12 mmol initiator). The flask was capped with a rubber septum and the contents were degassed by applying a vacuum and backfilling with argon three times. After modified MMT and HEMA (3.0 mL, 25 mmol) were mixed in the same tube, which had been degassed with bubbling argon for at least 45 min, they were added by syringe and placed in a thermostated oil bath and this suspension was stirred for 30 min. Another 10 mL Schlenk flask was charged with 0.0172 g (0.12 mmol) of CuBr and 0.0386 g of Bpy (0.241 mmol). The flask was capped. The contents were degassed by applying a vacuum and backfilling with argon three times. The solvent (70/30 v/v MEK/1-propanol; 3.0 mL) was added via syringe. This solution (transition metal catalyst complex) was transferred from this Schlenk flask to previous Schlenk flask (HEMA and modified MMT included) via cannula. The reaction mixture was stirred in a 55 °C oil bath for 1 h under nitrogen atmosphere. The polymergrafted MMT was precipitated in diethylether. The nanocomposite was collected and dried under vacuum.

F. Measurements

The molecular weight and molecular weight distributions of the polymers were determined with a gel permeation chromatograph (GPC). The GPC analyses were performed at 30 °C using N-methylpyrrolidinone as eluent at a flow rate of 0.5 mL/min. A differential refractometer was used as a detector. The instrument (Agilent 1100 series GPC-SEC system, Santa Clara, CA) was calibrated with a mixture of polystyrene standards (polysciences; molecular masses between 200 and 1,200,000 Da) using GPC software for the determination of the average molecular masses and the polydispersity of the polymer samples. Before the GPC measurement, the polymer was cleaved from clay by refluxing the nanocomposite in MEK/1-propanol solution (80/20, v/v) of *p*-toluenesulfonic acid for about 3 h, followed by centrifugation and filtration through a 0.2 μm filter.

Before the TGA measurements of the polymers, products, which have copper, were washed thoroughly with aqueous solution of disodium salt-ethylenediaminetetraacetic acid (EDTA) to remove the catalysts,[28] then precipitated with diethylether and dried in vacuum at 40 °C.

Transmission electron microscopy (TEM) analysis was carried out on a JEOL JEM-1200EX (Tokyo, Japan) electron microscope operated at 120 kV. TGA was performed on a Perkin Elmer Pyris 1 TGA instrument analyzer (Wellesley, MA) at a heating rate of 15 °C min^{-1} under a 1.5 bar air atmosphere between 50 and 750 °C. The measurement of T_g was performed on a Universal V4.3A TA Instrument DSC instrument (New Castle, DE). The differential scanning calorimetry (DSC) trace was recorded upon heating at a rate of 10 °C/min. All of the products were dried in a vacuum oven at 50 °C and 10 mbar. X-ray diffraction (XRD) patterns of the clay, the modified clay, and the polymer nanocomposites were collected on a Siemens D5000 θ/θ diffractometer (Germany) equipped with an intrinsic germanium detector system with Cu K_α radiation (λ: 1.5406 Å). Nuclear magnetic resonance (NMR) spectroscopy was performed on a Varian 300 spectrometer (Palo Alto, CA).

III. RESULTS AND DISCUSSION

An ammonium initiator was synthesized in a two-step procedure. As mentioned previously, the initiator synthesis was carried out in two steps: first by quaternization of amine group, and then the esterification of the product with 2-bromo-isobutyryl bromide. The resulting initiator was ion-exchanged onto MMT.

Modified MMT was identified via FTIR, TGA, and XRD. According to TGA diagrams (Fig. 4), unmodified MMT was found to have 8.53 wt% volatile materials. TGA of modified MMT reveals a silicate content of 22.8%, which corresponds to 63 mequiv immobilized initiator/100 g silicate. This value is lower than for the case of complete ion exchange because the cation exchange capacity (CEC) of the K10 is 100 mequiv/100 g.[29] CEC values for smectic clays are reported to range from 60 to 120 mequiv/100 g,[30,31] and the CEC value is 110 mequiv/100 g for MMT.[32] This smaller CEC value is attributed to the greater sterical demands of initiator compared to smaller inorganic ions.

If FTIR spectrum of the pristine MMT is compared with modified MMT, a new carbonyl peak can be easily seen at 1730 cm^{-1}, as shown in Fig. 5. This is a clear proof of the initiator modified MMT (K10).

Figures 6(a) and 6(b) display representative XRD patterns for MMT prior to and following modification, respectively. As indicated by Fig. 6 after ion exchange of clay with ATRP initiator, the interlayer distance increased from d_{001}~9.95 Å to d_{001} ~12.8 Å. This is indicative that the initiator penetrates to the interlayer region of MMT. The XRD pattern of the PHEMA/clay nanocomposite is shown in Fig. 6(c). The 001 diffraction peak of MMT did not appear in the XRD diagram, implying that the layered structure of the clay particles is largely destroyed as a result of the in situ polymerization process. However, because of the low content of the clay in the nanocomposite structure, XRD analysis might not be enough by itself to characterize this type of composites.

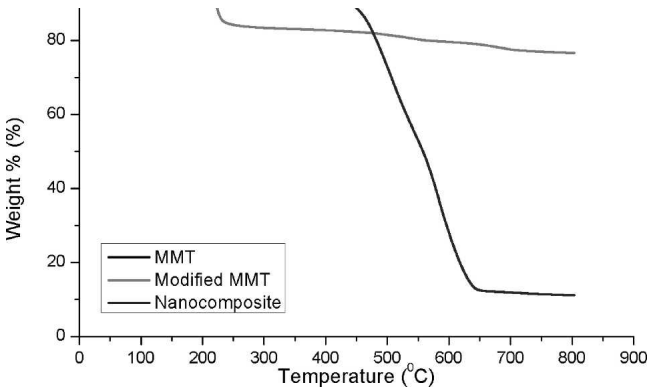

FIG. 4. TGA thermograms of unmodified MMT, modified MMT, and the nanocomposite.

Typical TEM micrographs of the nanocomposite are shown in Fig. 7. It was observed by analyzing the TEM images that exfoliated, intercalated, and stacked MMT platelets were present in the matrix. Exfoliated, intercalated, and stacked platelets (microcomposite) are represented, respectively, as Figs. 7(a), 7(b), and 7(c). From the images, it could be seen that some clay-rich sites were created in the nanocomposite matrixes. MMT (K10), which was acid treated, has attractive sites on its surfaces and edges, and the polymer as well. Because of these properties, strong interaction between MMT (K10) and PHEMA could take place. This affect could hinder the polymer chains from penetrating totally from matrix into inter-galleries of the clay.

The molecular weights were measured by GPC. In the first place, the nanocomposites should be purified. This purification was done in two steps. In the first step, the nanocomposite (100 mg) was suspended in MEK/1-propanol (150 mL), then *p*-toluenesulfonic acid (20 mg)

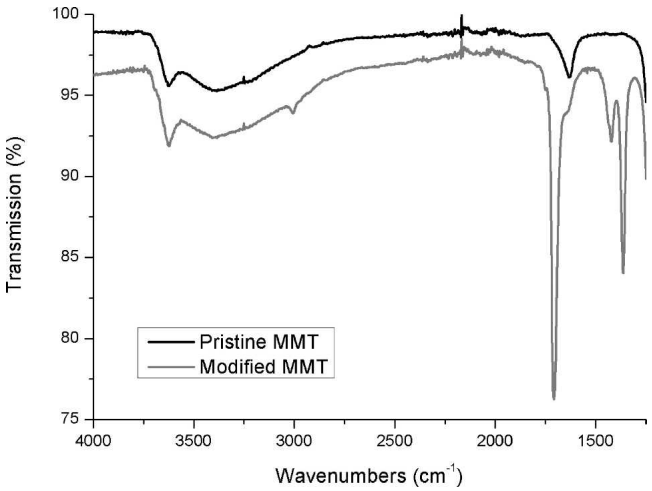

FIG. 5. FTIR spectrum of the unmodified and modified MMT (K10).

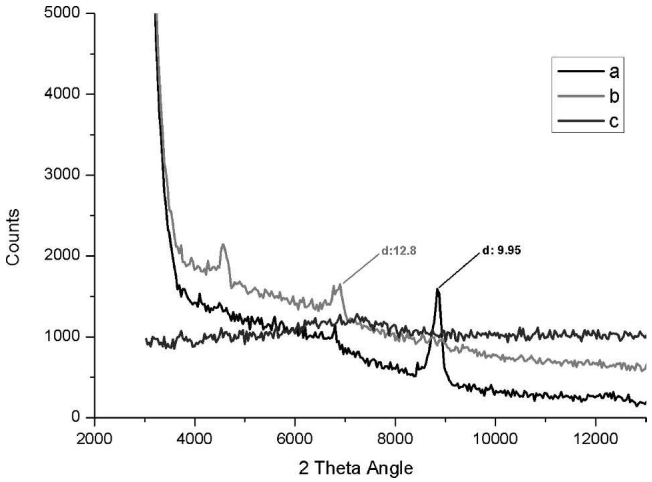

FIG. 6. XRD diagram of (a) MMT, (b) modified MMT, and (c) PHEMA/clay nanocomposite.

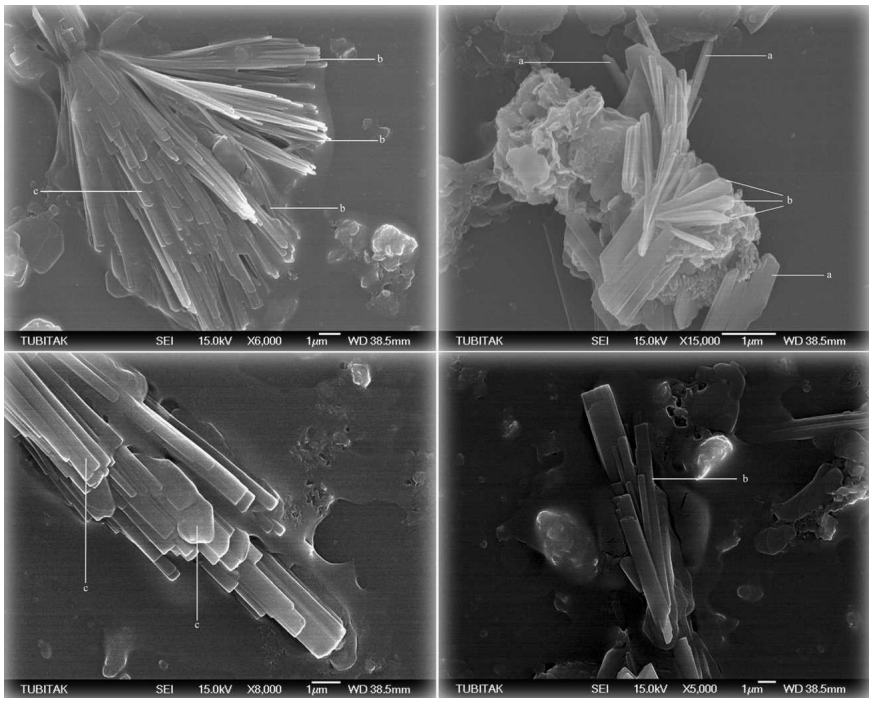

FIG. 7. Typical TEM micrographs of PHEMA-MMT nanocomposites.

was added, and the mixture was heated under reflux for 14 h. The mixture was transferred to centrifuge tubes, and the solid material was separated by centrifugation. The supernatant was collected by decantation, and the solution was eluted by a column of alumina. After that, the solution was concentrated under vacuum and the polymer was precipitated in diethyl ether medium. The polymer was filtered off and dried at 50 °C and 10 mbar to constant weight. According to GPC traces, the values of M_n of the PHEMA (synthesized with the BzO_2), pure PHEMA (synthesized via ATRP), and nanocomposite are, respectively, 100,000 (g mol^{-1}), 16,500 (g mol^{-1}), 10,500 (g mol^{-1}), and M_w/M_n ratios are 3.36, 1.40, and 1.30. There are primarily two kinds of polymers generated under different propagation conditions for ATRP polymerization; free polymer and bound polymer. In the case of modified clay initiated polymerization, the bound polymers grew with anchored initiators in inter galleries of clays. In contrast, the free polymer propagated from the free clay and the initiator is not bound to clay surfaces. For that reason, propagation is faster than in the case of a modified clay initiated situation.

According to the DSC characterization, the T_g temperature of the nanocomposite decreased slightly. While the T_g of the pure PHEMA (synthesized via ATRP) is 60.98 °C, that of the nanocomposite is 55.12 °C, i.e., T_g has decreased by 5.86 °C. High density regions might be formed in the nanocomposite structure because of some intercalating and stacking clay parts in the matrix. Stacking areas cause a decrease in T_g if the polymer-clay interaction is weak, and alternatively, the intercalating structures tend to increase the T_g value if the polymer-clay interaction is strong.[33] In the case of exfoliated structure, T_g does not change significantly.[34] Moreover, the molecular weight of the polymer, the particle size, the quantity of crosslink in polymer, the surface area and the polarity of polymer, and the filler can also affect the value of T_g. These parameters affect the polymer-clay interaction, mobility, and segmental motion of the polymer backbones, and the presence of intercalated, exfoliated, and microcomposite structures in the polymer matrix are consequences of these factors. The decrease in T_g leads to decreasing the energy consumption during polymer processing, such as molding and extruding.

The overall decomposition of PHEMA is known to consist of two kinds of reactions; one of them is the depolymerization to the monomer, which is the major reaction of low temperature decomposition. The other type of decomposition reactions takes place on the ester side chain and occurs at high temperatures.[35] In our studies, the TGA reveals that the inflection point of the nanocomposite in air is 45.9 °C higher than that of PHEMA (Fig. 8). The maximum temperatures of thermal degradation (inflection point) of the PHEMA (synthesized with the BzO_2), pure PHEMA (synthesized via ATRP), and nanocomposite are, respectively, 274.2, 268.74, and 314.65 °C in air. When similar investigation is done under N_2 atmosphere, the inflection point of the PHEMA (synthesized with the BzO_2), pure PHEMA (synthesized via ATRP), and nanocomposite were, respectively, 405.6, 400.95, and 408.75 °C.

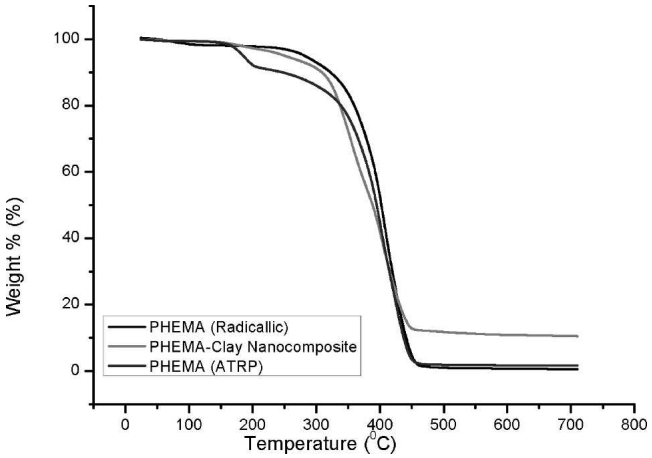

FIG. 8. TGA thermograms of PHEMA-nanocomposite, PHEMA (ATRP), and PHEMA (BzO_2).

The decomposition and degradation energies are shown in Table I. The decomposition energy of PHEMA-MMT (K10) nanocomposite decreased by 924.3 $J \cdot g^{-1}$ in air medium, and the degradation energy decreased by 120.0 $J \cdot g^{-1}$ in nitrogen medium. The nanocomposite exhibits a rather large increase in thermal stability as a result of the decrease in the exothermic degradation energies. The calculated activation energy of degradation using the Ozawa method[36] for PHEMA (ATRP) in air is 510.7 J mol^{-1}, and for PHEMA-MMT (K10) nanocomposite in air is 16453.2 J mol^{-1}. These results mean that the nanocomposite is more stable than the pure polymer. The stability of the PHEMA nanocomposite is commonly due not only to its different structure but also to restricted thermal motion of the PHEMA molecules in the gallery.[37]

In oxidative decomposition, the explanation for the improved thermal stability is char formation occurring under oxidative conditions. The char is reported to act as a physical barrier between the polymer and the superficial zone where the combustion of the polymer is running.[38] Other effects include heat barrier formed by the clay particles in the matrix and the declining gas diffusion properties because of the clay stacks; thus, if oxygen cannot penetrate, then it cannot cause oxidation of the polymer. Silicates are also known for their excellent thermooxidative stability and thereby provide a retarding effect on the thermal degradation of the organic component of the nanocomposites.[39] Therefore, the MMT (K10) should also enhance heat resistance of the phenolic resins of the nanocomposites.

TABLE I. Decomposition and degradation energies of PHEMA-nanocomposite, PHEMA (ATRP), and PHEMA (BzO_2).

Material	In air ΔH (J/g)	In nitrogen ΔH (J/g)
PHEMA (BzO_2)	−2148.5	−117.2
PHEMA (ATRP)	−2504.7	−127.0
PHEMA-MMT nanocomposite	−1580.4	−7.04

The explanation for the nonoxidative decomposition is similar to oxidative decomposition. The clay acts as a heat barrier, which enhances the overall thermal stability of the system, as well as assisting the formation of char after thermal decomposition.[39,40] In the early stages of thermal decomposition, the clay would shift the decomposition to higher temperatures. After that, this heat barrier effect would result in a reverse thermal stability. In other words, the stacked silicate layers could hold accumulated heat that could be used as a heat source to accelerate the decomposition process, in conjunction with the heat flow supplied by the outside heat source.[39] Gas diffusion is not expected to be as important as the oxidative case. For that reason, the change in thermal stability is smaller than the oxidative state.

To summarize, the TGA in this study reveals that the inflection point of the nanocomposite in air is 45.9 °C, higher than PHEMA. These results agree with the results of literature,[37,41] in which it was found that intercalated PMMA-MMT nanocomposites have a 40–50 °C higher decomposition temperature. Comparatively, the formation of Na-MMT microcomposite does not influence the thermal degradation of the polymer matrix both in air and nitrogen environments.[40] The dispersion of the clays is critical in increasing the degradation temperature. Delaminated composites have significantly higher degradation temperatures than intercalated nanocomposites or traditional clay composites.[42] Consequently, the obtained TGA results suggest that the intercalated structure in the polymer matrix is quite larger in quantity than exfoliated structure.

IV. CONCLUSIONS

The results show that the HEMA chains can be grown in the galleries of modified MMT with the bifunctional initiator 6-[(2-bromo-2-methylpropanoyl)oxy] hexan-1-aminium chloride at low reaction temperature (50 °C) through ATRP polymerization using the CuBr/bpy catalytic system.

TEM and XRD analysis showed the existence of microcomposite, intercalated, and exfoliated structures in the PHEMA-nanocomposite matrix, but as supported by TGA and DSC analysis, the majority of the clay structures in the matrix seem to be intercalated. The polydispersities were not high ($M_w/M_n \cong 1.3$), and the thermal degradation temperature of the polymer nanocomposite increased by 45.9 °C in air and 7.8 °C in N_2, whereas the T_g decreased by about 5.86 °C. Similarly, the degradation energies of PHEMA-clay nanocomposites decreased by 924.3 $J \cdot g^{-1}$ in air and 120.03 $J \cdot g^{-1}$ in nitrogen atmosphere. The activation energy of degradation according to

the Ozawa method[36] for PHEMA (ATRP) was calculated as 510.7 J mol^{-1} in air and was 16453.2 J mol^{-1} for PHEMA-MMT (K10) nanocomposite.

REFERENCES

1. P.B. Messersmith and S.I. Stupp: Synthesis of nanocomposites—Organoceramics. *J. Mater. Res.* **7,** 259 (1992).
2. A. Okada and A. Usuki: The chemistry of polymer-clay hybrids. *Mater. Sci. Eng., C* **3,** 109 (1995).
3. E.P. Giannelis: Polymer layered silicate nanocomposites. *Adv. Mater.* **8,** 29 (1996).
4. *Polymer-Clay Nanocomposites*, edited by T.J. Pinnavaia and G.W. Beall (Wiley, New York, 2000).
5. M. Alexandre and P. Dubois: Polymer-layered silicate nanocomposites: Preparation, properties and uses of a new class of materials. *Mater. Sci. Eng., R* **28,** 1 (2000).
6. M. Zanetti, S. Lomakin, and G. Camino: Polymer layered silicate nanocomposites. *Macromol. Mater. Eng.* **279,** 1 (2000).
7. M. Biswas and S.S. Ray: Recent progress in synthesis and evaluation of polymer–montmorillonite nanocomposites. *Adv. Polym. Sci.* **155,** 167 (2001).
8. J. Zhu, A.B. Morgan, F.J. Lamelas, and C.A. Wilkie: Fire properties of polystyrene–clay nanocomposites. *Chem. Mater.* **13,** 3774 (2001).
9. P.B. Messersmith and E.P. Giannelis: Synthesis and barrier properties of poly(e-caprolactone)-layered silicate nanocomposites. *J. Polym. Sci., Part A: Polym. Chem.* **33,** 1047 (1995).
10. M.S. Wang and T.J. Pinnavaia: Clay–polymer nanocomposites formed from acidic derivatives of montmorillonite and an epoxy resin. *Chem. Mater.* **6,** 468 (1994).
11. H.R. Fischer, L.H. Gielgens, and T.P.M. Koster: Nanocomposites from polymers and layered materials. *Acta Polym.* **50,** 122 (1999).
12. C. Zeng and L.J. Lee: Poly(methyl meacrylate) and polystyrene/clay nanocomposites prepared by in-situ polymerization. *Macromolecules* **34,** 4098 (2001).
13. X. Huang and W. Brittain: Synthesis and characterization of PMMA nanocomposites by suspension and emulsion polymerization. *Macromolecules* **34,** 3255 (2001).
14. D.Y. Wang, J. Zhu, Q. Yao, and C.A. Wilkie: A comparison of various methods for the preparation of polystyrene and poly(methyl methacrylate) clay nanocomposites. *Chem. Mater.* **14,** 3837 (2002).
15. T.J. Pinnavaia: Intercalated clay catalysts. *Science* **220,** 365 (1983).
16. M. Alexandre and P. Dubois: Polymer-layered silicate nanocomposites: Preparation, properties and uses of a new class of materials. *Mater. Sci. Eng., R* **28,** 1 (2000).
17. K.A. Carrado and L.Q. Xu: In-situ synthesis of polymer ± clay nanocomposites from silicate gels. *Chem. Mater.* **10,** 1440 (1998).
18. E.P. Giannelis: Polymer layered silicate nanocomposites. *Adv. Mater.* **8,** 29 (1996).
19. P.B. Messersmith and E.P. Giannelis: Synthesis and barrier properties of poly(e-caprolactone)-layered silicate nanocomposites. *J. Polym. Sci., Part A: Polym. Chem.* **33,** 1047 (1995).
20. G.B. Rossi, G. Beaucage, T.D. Dang, and R.A. Vaia: Bottom-up synthesis of polymer nanocomposites and molecular composites: Ionic exchange with PMMA latex. *Nano Lett.* **2,** 319 (2002).
21. M.W. Weimer, H. Chen, E.P. Giannelis, and D.Y. Sogah: Direct synthesis of dispersed nanocomposites by in situ living free radical polymerization using a silicate-anchored initiator. *J. Am. Chem. Soc.* **121,** 1615 (1999).
22. H. Böttcher, M.L. Hallensleben, S. Nuss, H. Wurm, J. Bauer, and P. Behrens: Organic/inorganic hybrids by 'living'/controlled ATRP grafting from layered silicates. *J. Mater. Chem.* **12,** 1351 (2002).
23. S. Su and C.A. Wilkie: Exfoliated poly(methyl methacrylate) and polystyrene nanocomposites occur when the clay cation contains a vinyl monomer. *J. Polym. Sci., Part A: Polym. Chem.* **41,** 1124 (2003).
24. X. Tong, H. Zhao, T. Tang, Z. Feng, and B. Huang: Preparation and characterization of poly(ethyl acrylate)/bentonite nanocomposites by in situ emulsion polymerization. *J. Polym. Sci., Part A: Polym. Chem.* **40,** 1706 (2002).
25. J. Zhu, P. Start, K.A. Mauritz, and C.A. Wilkie: Silicon-methoxide-modified clays and their polystyrene nanocomposites. *J. Polym. Sci., Part A: Polym. Chem.* **40,** 1498 (2002).
26. Q. Zhou, X. Fan, C. Xia, J. Mays, and R. Advincula: Living anionic surface initiated polymerization (SIP) of styrene from clay surfaces. *Chem. Mater.* **13,** 2465 (2001).
27. K.L. Beers, S. Boo, S.G. Gaynor, and K. Matyjaszewski: Atom transfer radical polymerization of 2-hydroxyethyl methacrylate. *Macromolecules* **32,** 5772 (1999).
28. H.B. Sonmez, B.F. Senkal, D.C. Sherrington, and N. Bicak: Atom transfer radical graft polymerization of acrylamide from N-chlorosulfonamidated polystyrene resin, and use of the resin in selective mercury removal. *React. Funct. Polym.* **55,** 1 (2003).
29. K. Yamaoka, R. Sasai, and N. Takata: Electric linear dichroism. A powerful method for the ionic chromophore–colloid system as exemplified by dye and montmorillonite suspensions. *Colloids Surf., A* **175,** 23 (2000).
30. C.D. Shackelford, C.H. Benson, T. Katsumi, T.B. Edil, and L. Lin: Evaluating the hydraulic conductivity of GCLs permeated with non-standard liquids. *Geotext. Geomembr.* **18,** 136 (2000).
31. S.S. Ray and M. Okamoto: Polymer/layered silicate nanocomposites: A review from preparation to processing. *Prog. Polym. Sci.* **28,** 1550 (2003).
32. S.S. Ray, K. Okamoto, and M. Okamoto: Structure–property relationship in biodegradable poly(butylene succinate)/layered silicate nanocomposites. *Macromolecules* **36,** 2355 (2003).
33. C. Becker, P. Mueller, and H. Schmidt: Optical and thermomechanical investigations on thermoplastic nanocomposites with surface-modified silica nanoparticles. *SPIE* **88,** 3469 (1998).
34. P.M. Ajayan, L.S. Schadler, and P.V. Braun: *Nanocomposite Science and Technology* (Wiley-VCH Verlag GmbH & Co., KGaA, Weinheim, Germany, 2003), p. 96.
35. K. Demirelli, M. Coşkun, and E. Kaya: A detailed study of thermal degradation of poly(2-hydroxyethyl methacrylate). *Polym. Degrad. Stab.* **72,** 75 (2001).
36. T. Ozawa: A new method of analysing thermogravimetric data. *Bull. Chem. Soc. Jpn.* **38,** 881 (1965).
37. S.S. Ray and M. Okamoto: Polymer/layered silicate nanocomposites: A review from preparation to processing. *Prog. Polym. Sci.* **28,** 1605 (2003).
38. G. Beyer: Nanocomposites: A new class of flame retardants for polymers. *Plast. Additives & Compound.* **4**(10), 26 (2002).
39. S.S. Ray and M. Okamoto: Polymer/layered silicate nanocomposites: A review from preparation to processing. *Prog. Polym. Sci.* **28,** 1607 (2003).
40. M. Alexandre and P. Dubois: Polymer-layered silicate nanocomposites: Preparation, properties and uses of a new class of materials. *Mater. Sci. Eng.* **28,** 52 (2000).
41. M. Alexandre and P. Dubois: Polymer-layered silicate nanocomposites: Preparation, properties and uses of a new class of materials. *Mater. Sci. Eng.* **28,** 55 (2000).
42. P.M. Ajayan, L.S. Schadler, and P.V. Braun: *Nanocomposite Science and Technology* (Wiley-VCH Verlag GmbH & Co., KGaA, Weinheim, Germany, 2003), p. 136.